Master thesis

2D simulation of rf-discharges

Submitted by: Paul Matthias
Born at: 15.05.1990, Greifswald

Reviewer: Prof. Dr. Ralf Schneider
Prof. Dr. Jürgen Meichsner

Submitted at: March 21, 2017

Contents

1 Introduction

Capacitive-coupled discharges with a radio-frequency modulated voltage are important for plasma etching [1] and sputter processes [2].

The latest results of an experiment with electronegative discharges have shown a high-energy peak of the negative ions arriving at the anode, depending on the cathode material used. One possible explanation is ionization at or close to the surface for the production of negative ions.

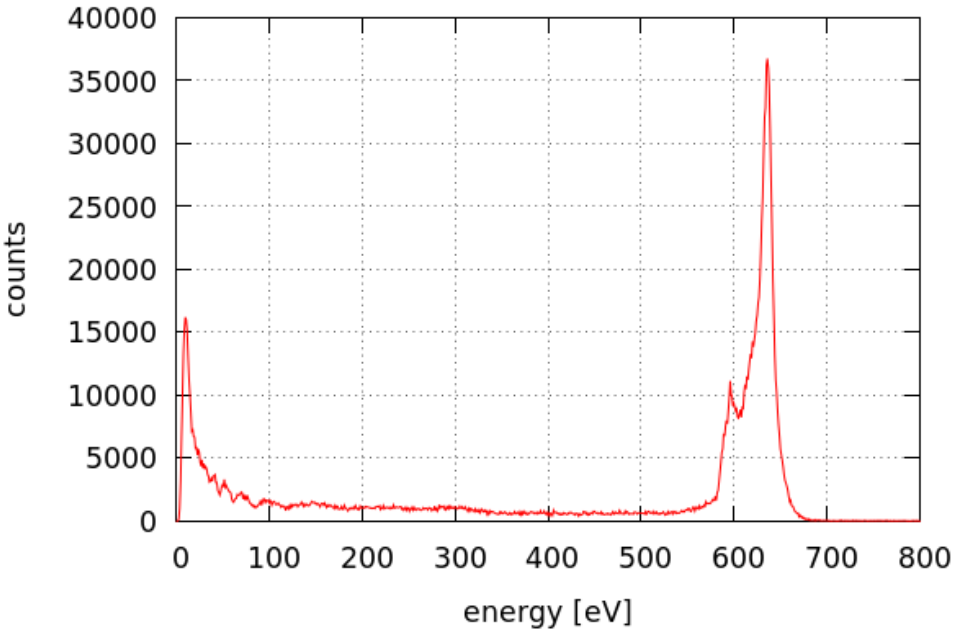

Figure 1.1: Experimental measured negatively charged oxygen ions arriving at the grounded anode as shown in [3]. The cathode material used was Magnesiumoxide (MgO) and the cathode was powered with 50 W.

I want to improve the insight into microscopic mechanisms of electronegative plasmas and surface ionization effects using a MCC-PIC simulation.

1.1 Surface effects and secondary ion emission

In comparison to the known secondary electron emission there also exists **s**econdary **i**on **e**mission (SIE). Theoretical studies of surface ionization are mostly devoted to the production of positive ions from incident atoms having thermal energies [4]. The degree of

ionization can be derived by applying thermodynamic arguments. The ionization coefficient of M is then given by

$$\begin{aligned}\alpha^+(M^+) &= \frac{n^+}{n} \\ &= \frac{1-r^+}{1-r}\cdot\frac{w^+}{w}\exp\left(\frac{\bar{\Phi}^+ + e\sqrt{eF} - I(M)}{k_B T}\right) ,\end{aligned} \tag{1.1}$$

where n^+ and n are the numbers of M^+ and M coming from unit surface area per unit time, w^+/w is the statistical weight ratio of M^+ to M, r^+ and r are the internal reflection coefficients at the potential barrier on the emitter surface, $\bar{\Phi}^+$ is the average work function, T is the absolute temperature at the surface, F is the externally applied field and $I(M)$ is the initial energy of the impinging atoms.

With little adaptations I can transfer equation (1.1) for treating a surface which emits negative ions. I assume a negatively biased surface like the cathode in an asymmetric ccrf discharge where the equilibrium

$$X + e^- \text{ (in the substrate metal)} \leftrightharpoons X^- \tag{1.2}$$

is attained at the surface. Hence, the equation for the negative ionization coefficient follows in analogy to equation (1.1)

$$\begin{aligned}\alpha^-(X^-) &= \frac{n^-}{n} \\ &= \frac{1-r^-}{1-r}\cdot\frac{w^-}{w}\exp\left(\frac{-\bar{\Phi}^- + e\sqrt{eF} + A(X)}{k_B T}\right) ,\end{aligned} \tag{1.3}$$

where $A(X)$ is the electron affinity of atom X, $\bar{\Phi}^-$ is the average work function effective for producing the negative ion X^- on the metal surface and the other parameter are in analogy to the positive ion injection. To the best of my knowledge. there are no detailed theoretical and experimental studies of the reflection coefficients r for negative ions.
Therefore no detailed information about the cross-sections for such processes exists. In this work I assume that negative ions are produced by a positive ion beam on the surface with an efficiency of $\eta = n_-/n_+$.
The additional flux of negatively charged particles leads to a reduction of the potential drop as in the case of secondary electron emission.

To get a microscopic knowledge of a ccrf discharge the discharge is simulated. Since nonthermal low pressure plasmas are not collision dominated the particles are not Maxwell distributed. The mean free paths are of the same magnitude as the electrode gap. This means that fluid models fail at this point and kinetic models have to be applied. I will use the PIC-MCC method which is widely used for plasma simulation.

1.2 PIC-MCC

1.2.1 1d3v PIC

The discharge of the experiment has a cylindrical geometry. In the centre of the discharge the plasma does not see the edge of the electrodes and therefore no asymmetry effects may take place. For the middle of the discharge it is sufficient to do an one-dimensional approach. The disadvantage of the 1d3v simulation is the neglect of different transport processes in radial direction. This leads to a discrepancy between simulation and real experiment. I adjust my parameters in a way so that I receive comparable results close to one electrode, where the experimental measurements took place. In this case I cannot compare absolute values but can still see trends in the distribution functions.
I can compare these results with a 2d3v simulation. This will separate the asymmetric influence.

1.3 Experimental setup

Experimental results from the group of Professor Meichsner are used. The experimental setup is shown in figure (1.2). It shows a schematic plasma chamber from above. The plasma apparatus consists of a cylindrical vacuum chamber built of stainless steel. At the cathode a rf voltage of frequency 13.56 Hz and a voltage of (500-2000) V is applied. The anode and the casing are both grounded. The distance between the electrodes is varied between (3-5) cm. The difference of the area of the cathode to the grounded anode in addition to the grounded wall leads to an asymmetric discharge characterized by a negative DC self-bias voltage at the powered electrode. The pressure is set up to (2-10) Pa and the process gas is oxygen O_2. To detect ions O^- at the anode a mass spectrometer is attached. Additionally, a PROES (**P**hase **r**esolved **o**ptical **e**mission **s**pectroscopy) diagnostic is applied.

By applying a voltage to the cathode a plasma develops. The basics of ccrf plasma physics are described in chapter (**??**). The cold positive ions O_2^+ of the bulk get accelerated at the plasma sheath towards the grounded anode. There they are detected by the mass spectrometer and result in a well known distribution [5] as shown in figure (1.3). The incoming negative ions O^- are detected as well. The number of detected negative ions is much lower than the number of detected positive ions. The negative ion distribution of stainless steel and magnesium oxide in figure (1.4) show a low-energy peak followed by a plateau which proceeds up to very high energies of several 100 eV.
Depending on the cathode material a high-energy peak appears in the negative ion distribution.

In this experiment different materials have been tested (SiO_2, Al_2O_3, magnesium oxide (MgO), stainless steel). In the following I use a PIC simulation to test if these ions originate from surface processes at the cathode or if they emerge from asymmetry effects.

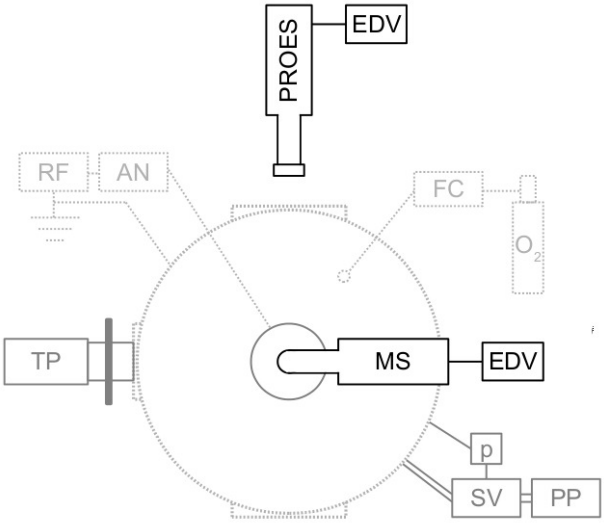

Operating parameter:

frequency :	13.56 MHz
power :	7...51 W
pressure :	4...10 Pa
process gas :	O_2
material of electrode :	stainless steel, SiO_2, Al_2O_3, MgO

Figure 1.2: Top view of the schematic experimental setup taken from [3].

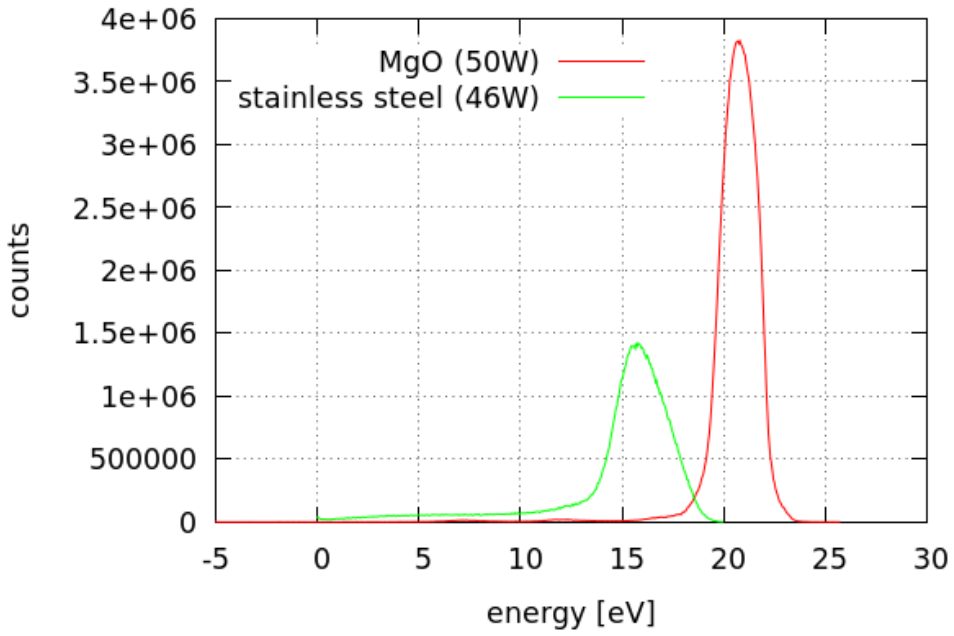

Figure 1.3: Comparison of the positive ion energy distribution for stainless steel and magnesium oxide.

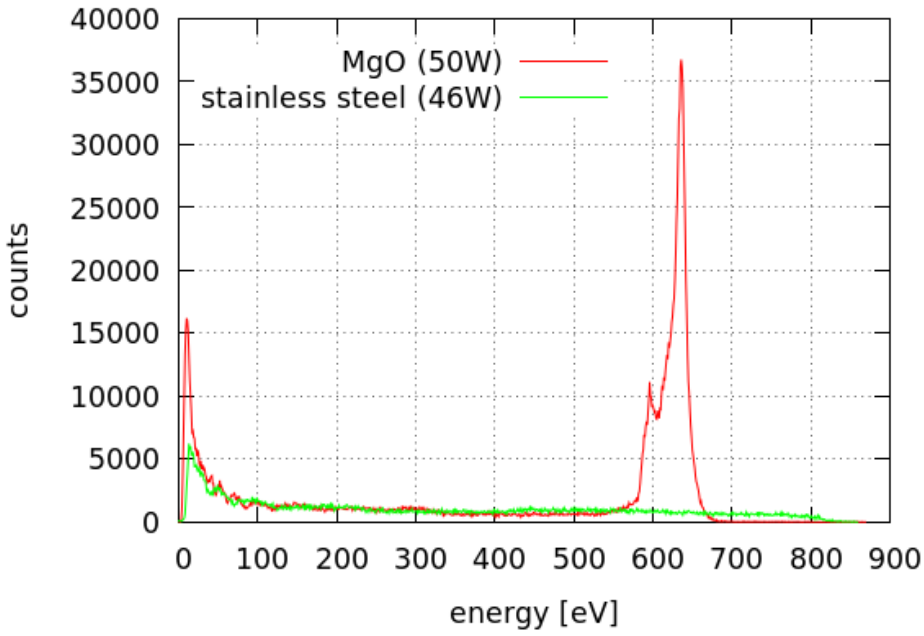

Figure 1.4: Comparison of the negative ion energy distribution for stainless steel and magnesium oxide.

2 PIC simulation of a ccrf discharge

The system starts with a pressure of 10 Pa and a peak-to-peak voltage of 800 V. From there on the pressure will be reduced to get to low pressures around 2 Pa. The radio-frequency is set to 13.56 MHz. The initial values for the considered electron density $n_e = 5 \cdot 10^9 \,/\mathrm{cm}^{-3}$ and electron temperature $T_e = 4\,\mathrm{eV}$ are set.
The Debye-length of the system is $\lambda_{Db} \approx 0.021\,\mathrm{cm}$ and the electron plasma frequency is $\omega_{pe} \approx 3.99 \cdot 10^9\,\mathrm{s}^{-1}$. The electrode gap of the experiment is 5 cm. To obtain a comparable plasma in 1D the simulation was done with a domain length of 6.72 cm.
The results for low pressure discharges do not give us an explanation for the measured high-energy peak (s. figure 1.4).

2.1 Discharge with secondary ion emission

After I implemented the proposed SIE injection model of oxygen anions, one can see in figure (2.1) that the number density of the anions is higher and slightly shifted towards the cathode. Here, I chose the injection coefficient $\eta = 0.03$.

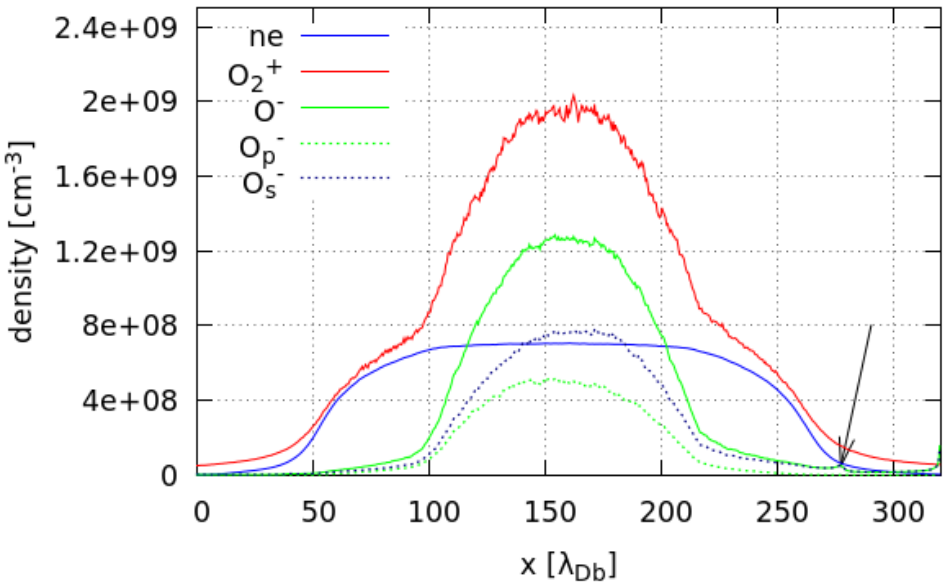

Figure 2.1: Density distribution of e^-, O_2^+ and O^- with secondary ion emission at the cathode ($\eta = 0.03$). The pressure was 5 Pa and the rf power was set to $U_{rf} = 800\,\mathrm{V_{pp}}$. The arrow marks the little density peak of O_s^- at the cathode sheath edge.

Since I want to study the behavior of the anions coming from the surface I separated the two species. I refer to them as anions produced by volumetric processes in the plasma O_p^- and surface anions O_s^-.

It is visible that the density distribution of O_s^- is of one magnitude higher than O_p^-. This depends on the chosen injection ratio η. The surface ion density has a peak close to the cathode resulting from the injection of O_s^-. In addition a small density peak at the sheath edge in front of the cathode is noticeable. It forms due to elastic collisions of the anions O_s^- in the sheath.
The O_s^- get accelerated in the sehat, cross the bulk and then get reflected in the anode sheath similar to electrons.

With additional SIE a high-energy peak builds up. It decays with the time of flight (distance to the cathode) due to charge-exchange and elastic collisions with neutral molecules O_2 which results in an energy loss for the anion. Also a part of the anions gets detached by neutrals or recombines with positive ions. Until now it was assumed that if an anion collides with a neutral it almost gets detached every time. But the anions also do elastic collisions which leads to an energy loss and a plateau in the energy. In figure (2.3) the difference between the numbers of elastic collisions for a normal discharge and a discharge with additional SIE are shown. Most elastic collisions happen in the bulk while the sheaths

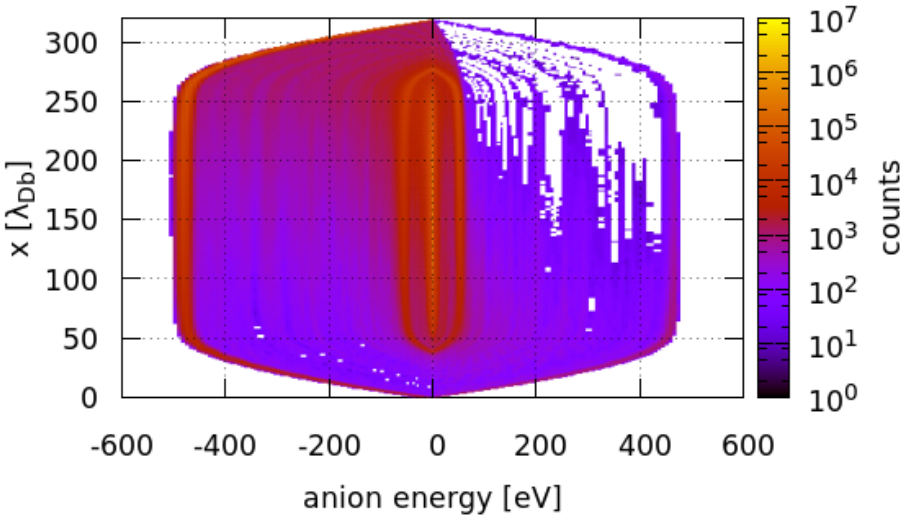

Figure 2.2: Energy distribution of O_s at 5 Pa.

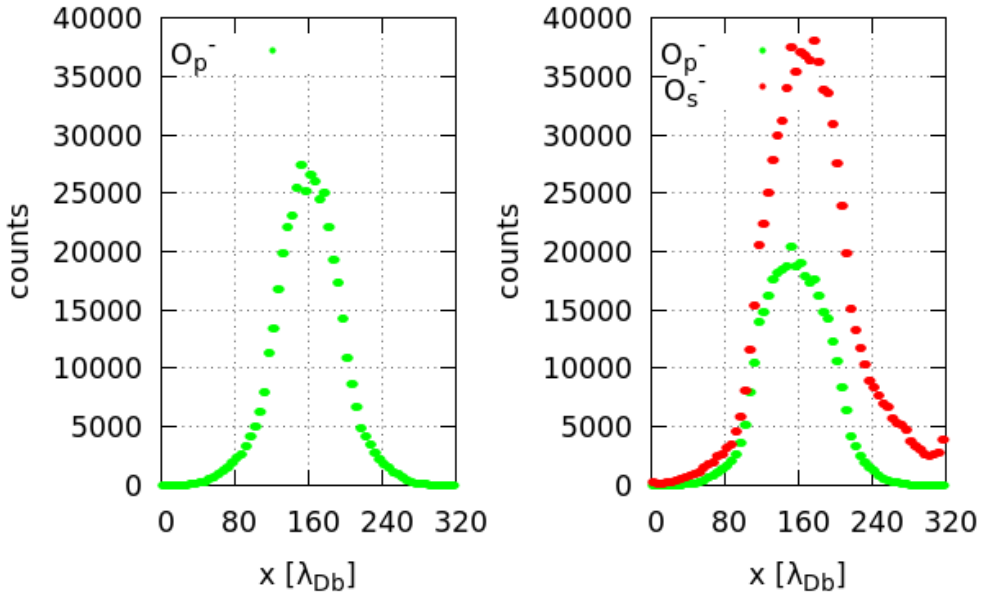

(a) (b)

Figure 2.3: Number of elastic collisions of negative ions O^- with neutral molecules O_2 per 10^5 steps. The figure shows them in simulation without SIE (a) and with SIE ($\eta = 0.03$) (b) where between the two O^- species is differentiated.

are mostly collisionless. But for the surface ions O_s^- one can see that the collisions in the cathode sheath cannot be neglected. They lead to an energy loss for the anions which impacts on their energy distribution.
In figure (2.2) a structure in the lower energy area can be seen. The performed elastic collisions during this phase lead to a peak structure in the ion energy distribution. To get an impression of the dynamics in the sheath the phase resolved energy distribution for O_s^- is shown in figure (??)).

The density peak at the sheath edge (as seen in figure (2.1)) originates from the low-energy peak in the energy distribution. With the approximate transit time of an anion τ_{ion} and the rf-cycle time τ_{rf} one can calculate the transit time τ_{ion}. Assuming an average ion energy of $40 - 50\,\mathrm{eV}$ and a traveled distance of $\approx 1\,\mathrm{cm}$ it follows the ratio $\frac{\tau_{ion}}{\tau_{rf}} \approx 4.5$. This is the number of rf cycles an anion stays in the sheath. Hence the number of peaks in the ion energy distribution must be similar. In figure (??) one can see a high-energy peak and 4-5 low-energy peaks in the bulk region. At the sheath edge these density waves overlay. Hence, the energy plateau of the anions is mainly influenced by elastic collisions. This explains the density peak at the sheath edge. In the experiment where the cathode potential is shifted by the self-bias voltage the resulting potential is asymmetric. That means, the anions can get enough energy to get to the anode while in the current simulation due to the forced symmetry they get reflected by the sheath potential. Figure (2.5) confirms that negative ions produced at the surface may lead to the measured high-energy peak. But the energy distribution function of the simulation has additional low energy peaks (at $< 100\,\mathrm{eV}$), too. I consider them to be created due to the lack of asymmetry in the simulation. In the experiment all high-energy anions are detected and thereby removed of the discharge.
Additional studies have been done considering variation of pressure, voltage and injection coefficient. These studies all support the alredy proposed thesis.

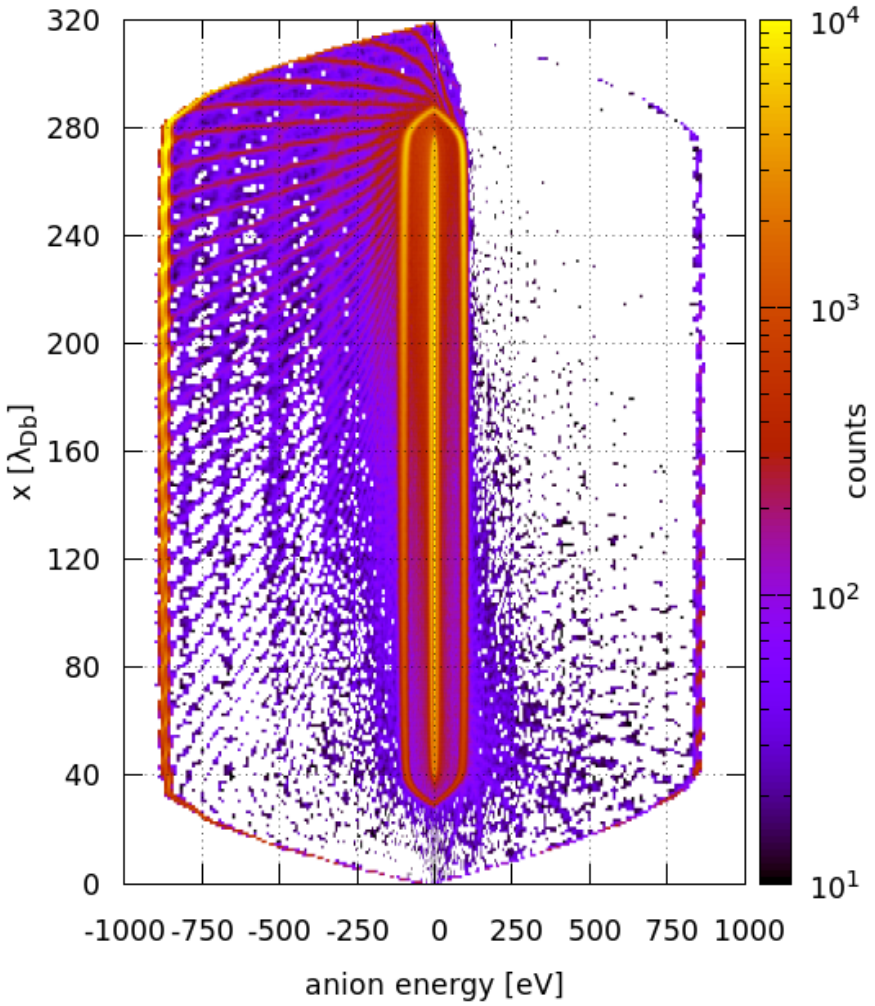

Figure 2.4: Same energy distribution as in figure (2.2) at t=0 of the rf cycle, which is equal to $U(t) = 0$.

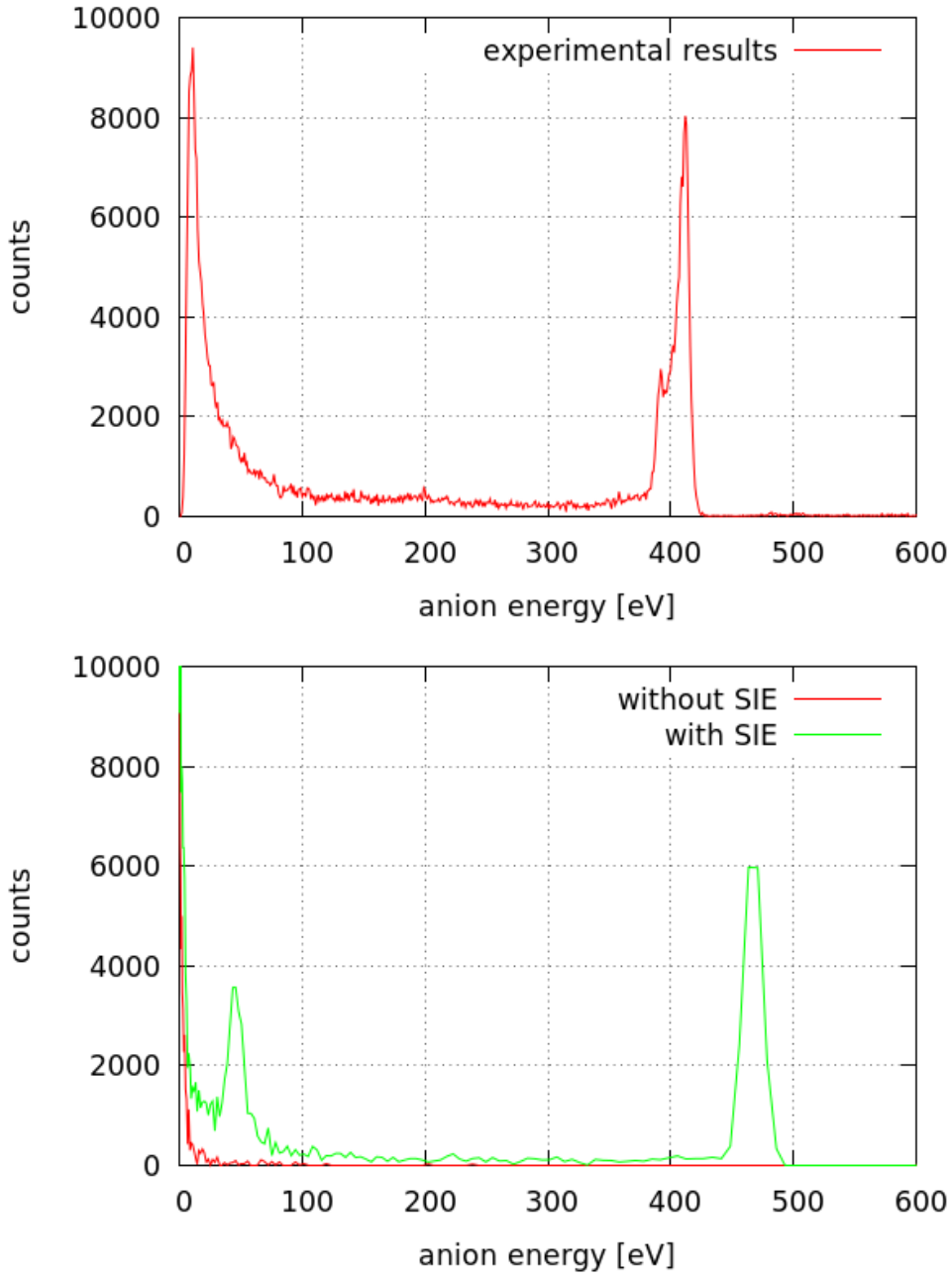

Figure 2.5: Energy distribution of negative ions O^-. Top: Experimental results for MgO measured at the anode for different rf powers. Bottom: Simulation result with 1d3v PIC simulation with additional SIE taken at the anode sheath edge.

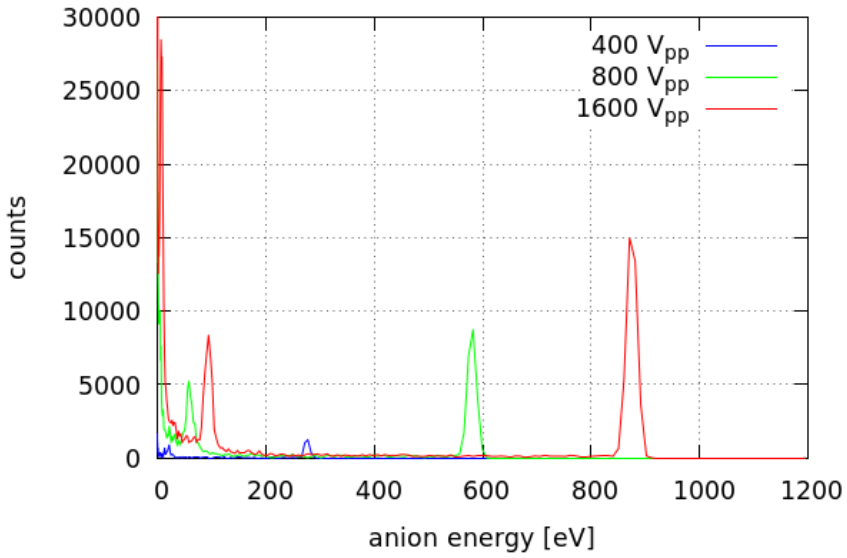

Figure 2.6: O_s^- energy distribution under different driver voltages U_{rf} with 5 Pa and $\eta = 0.01$.

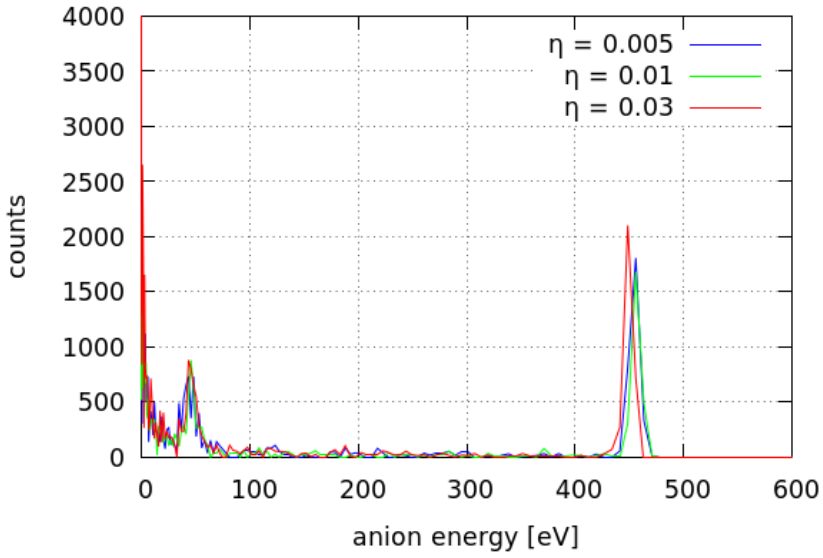

Figure 2.7: O_s^- energy distribution for different η with 5 Pa and $U_{rf} = 800V_{pp}$.

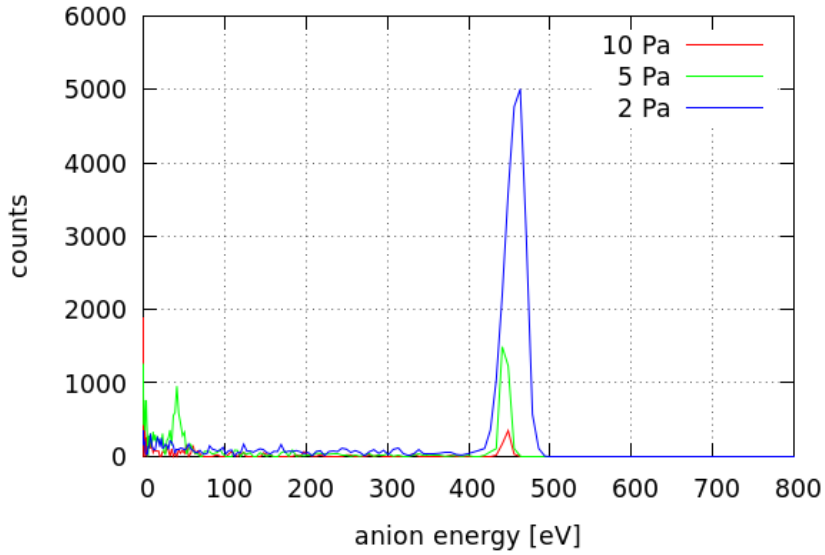

Figure 2.8: O_s^- energy distribution under different pressures with $U_{pp} =$ V and $\eta = 0.01$.

3 Two-Dimensional PIC simulation

The two-dimensional PIC code used was developed by the group of Prof. Dr. Ralf Schneider. Over several years the code was developed and optimized for ion thruster modeling. I adapted it to simulate a capacitively coupled rf discharge.
Due to the symmetry of the discharge a cylindrical geometry in r and z direction is used.

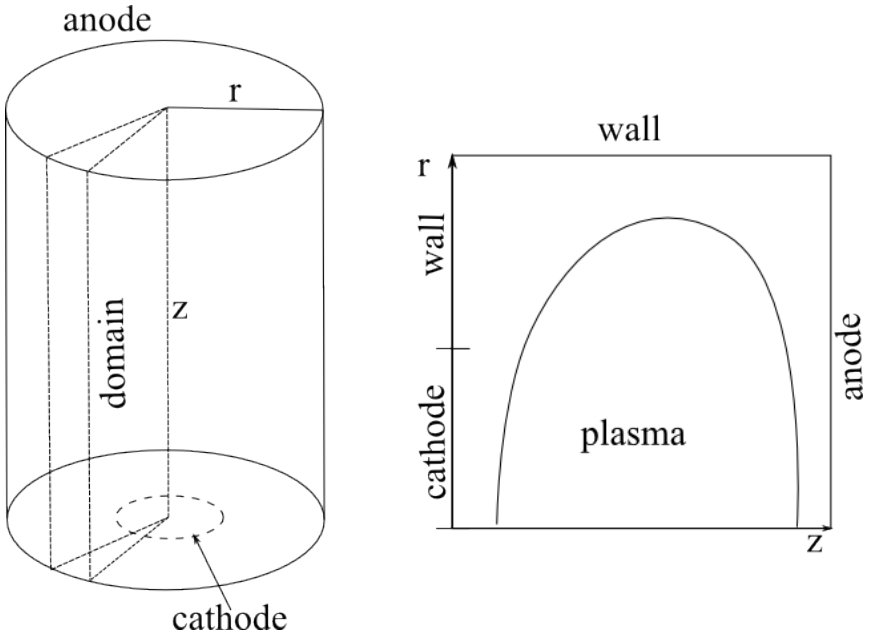

Figure 3.1: Schematic figure of the geometry of the discharge. On the left hand side is shown the whole discharge in a cylinder, where the simulation domain is marked as a slice. On the right hand side the resulting domain with the corresponding boundary conditions is shown.

To realize an asymmetric discharge the size of the cathode is set smaller than the size of the anode. This in addition to the grounded wall leads to a strong asymmetry. In an asymmetric discharge the high mobility of the electrons charges the cathode, which then gets a negative self-bias voltage.

3.1 Simulation of an asymmetric ccrf discharge

A bigger domain size (500x200), which gets closer to the experimental size, is used from now on. In the following simulations with an asymmetry factor of 0.6 will be used, resulting in a cathode radius of $\approx 2.5\,\mathrm{cm}$. In figure (3.2) the averaged potential is shown. Due to the asymmetry a negative self-bias voltage at the cathode builds up. This is a main

difference to one-dimensional simulations. To compare the potential with one-dimensional simulations (s. figure (**??**)) one has to look at the potential at the axis nr=0 (s. figure (3.3)). The shape is the same despite the self-bias voltage which shows the advantage of two-dimensional simulations to obtain a realistic potential.

HERE PUT NEW PIC OF POTENTIAL!!!1

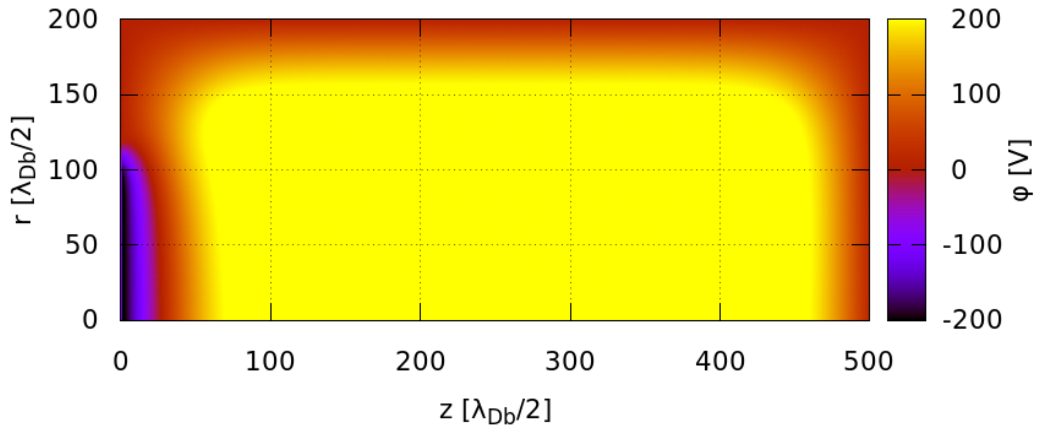

Figure 3.2: Potential of an argon rf discharge with an asymmetry ratio of 0.6. This leads to a cathode size of $r_{cathode} \approx 2.5\,\mathrm{cm}$. The pressure was set to 30 Pa and the power was $U_{rf} = 1000\,\mathrm{V_{pp}}$.

In figure (3.4) the electron and ion number density after a runtime of 30 rf cycles after initialization are shown. This is a not yet fully equilibrated state of the plasma, due to the long run-times. One can see that the bulk region is slightly deformed at the cathode side. This is due to the self-bias voltage which leads to a reduced electron flux towards the cathode. The ions follow the motion of the electrons.

Now the density distribution can be compared with the previous one-dimensional results. Therefore, the number density distributions of the charged species at the axis (s. figure (3.6)) are taken, which equals the one-dimensional domain.

One can see the quasi-neutral bulk region and the ion flux towards the walls. There is a higher flux of ions towards the cathode than to the anode due to the self-bias voltage. This additional flux is not covered by the one-dimensional simulation. Additionally, the cathode sheath is larger in two dimensions, due to the self-bias voltage. So in a one-dimensional simulation the total ion flux towards the cathode and the cathode sheath width are slightly underestimated. Nevertheless, the form of the number density distributions is nearly the same, which shows that a one-dimensional simulation is a good approximation regarding the number densities for capacitively discharges near the center.

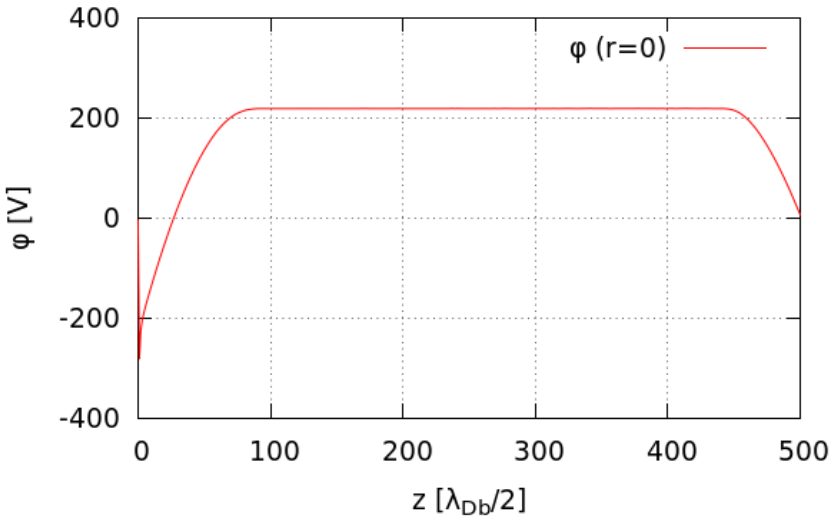

Figure 3.3: Potential of an argon discharge at the axis ($r = 0$).

In addition to the density distributions and the potential a closer look at the energy distributions of the plasma particles is taken. The ion energy distributions in r and z direction are shown in figure (3.7) and (3.8). The z component of the ion energy distribution shows the expected behavior of cold ions in the bulk and accelerating ions towards the electrodes (s. figure (3.7 (a))), when averaged along r at fixed z. The radial component of the ion energy distribution (s. figure (3.8)) shows the same acceleration of the ions towards the wall. Near the cathode edge (r=120) the ions are accelerated towards the cathode due to the radial potential gradient, which results in a larger ion energy.
When comparing the electron energy distributions with the results from the one dimensional PIC simulation (s. figure (**??**)), one can see that for the z component of the electron energy distribution (s. figure (3.9 (a))) the shape of the distributions is nearly the same, except near the cathode. Due to the asymmetry the potential has additional radial gradients, especially above the cathode (s. figure (3.2)). This leads to a shift in the electron energy distribution function near the cathode, where the electrons get pushed in radial direction. In the experiment the cathode usually is not located at the wall, but stands in free space. Here the cathode is embedded in a grounded ring. So this is an effect which can be modified by moving the cathode into the domain. Then the mesh and the boundary conditions have to be applied accordingly. But I am not doing this approach in this thesis. Naturally, the r component of the electron distribution function is affected by the same radial gradient of the potential and builds up an analogue distribution function (s. figure (3.10)).

Now that I achieved a stable argon discharge in a two dimensional PIC simulation the next step would be to simulate an oxygen plasma and apply the proposed SIE processes. The runtime for in depth studies of even larger domains exceeds the time limit of this thesis. But the two dimensional system is prepared for capacitively coupled rf plasmas and future research may continue this approach.

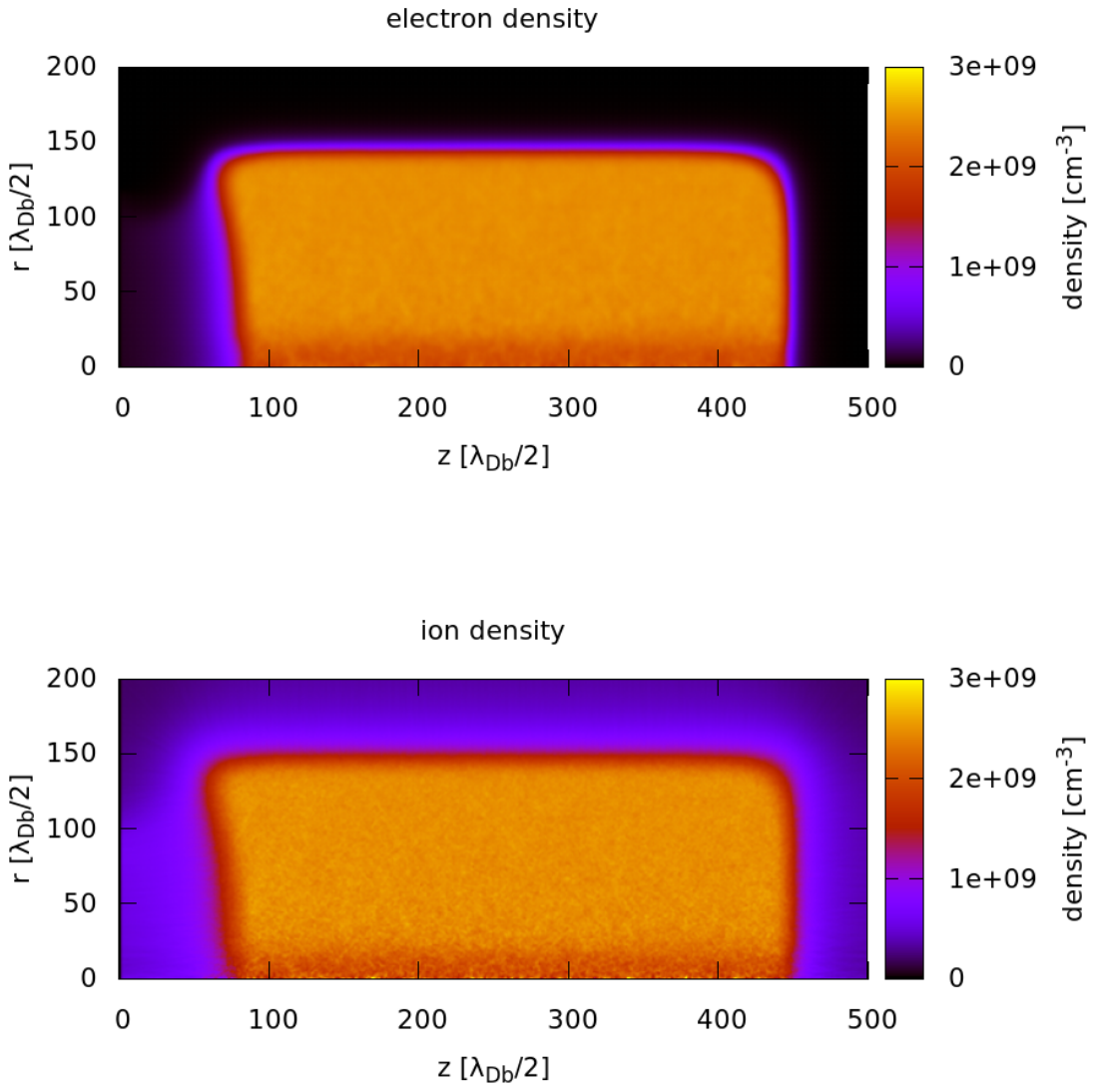

Figure 3.4: Charged particle density distribution of an argon discharge.

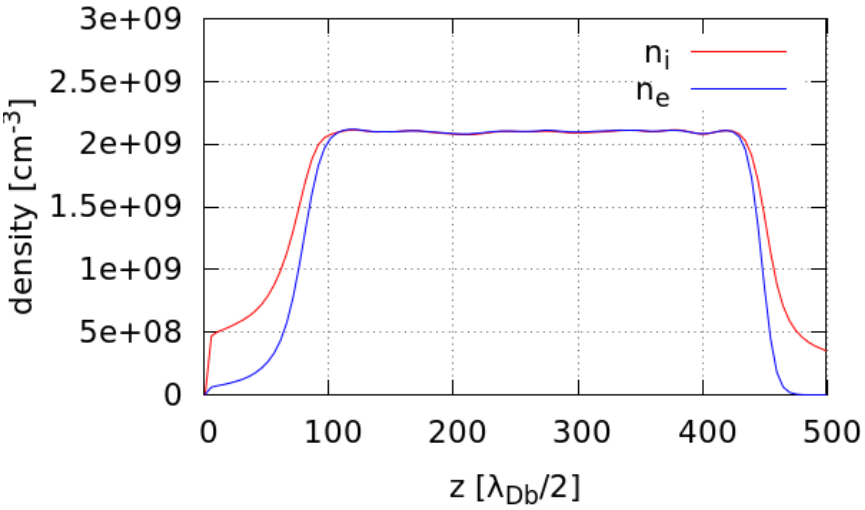

Figure 3.5: Charged particle density distribution of an argon discharge at the center of the discharge from a two-dimensional PIC simulation at 30 Pa and 1000 V_{pp}.

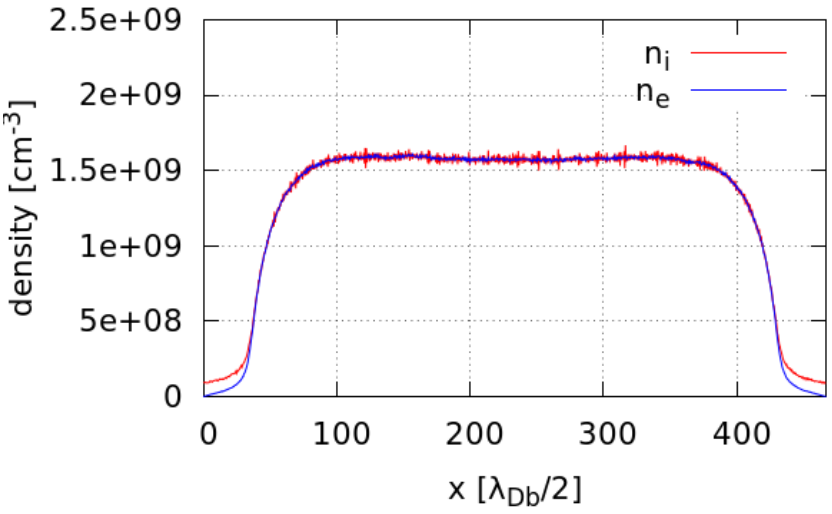

Figure 3.6: Charged particle density distribution of an argon discharge out of an one-dimensional PIC simulation at 30 Pa and 400 V_{pp}.

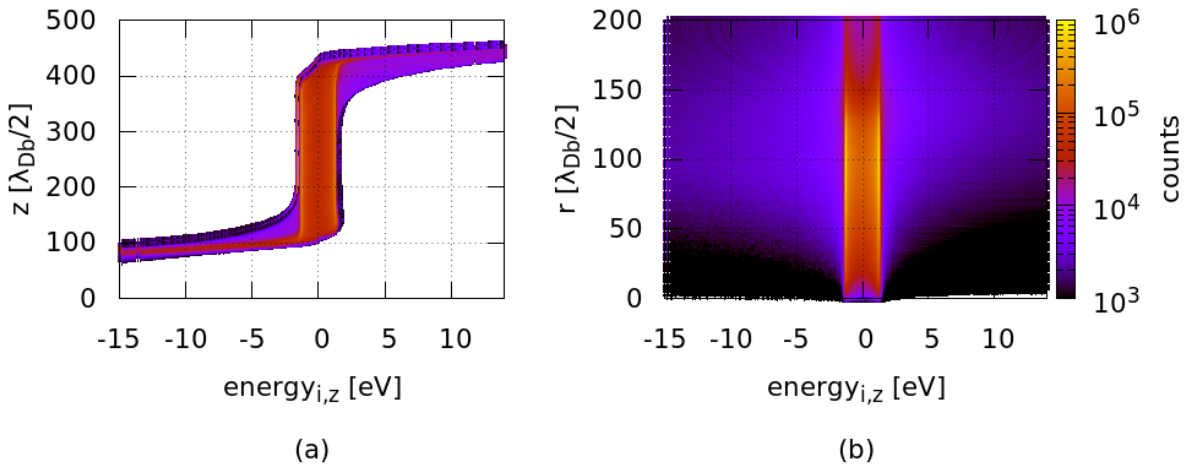

Figure 3.7: Ion energy distribution in z direction. (a) shows the averaged energy resolved for the vertical z axis and (b) for the radial r axis

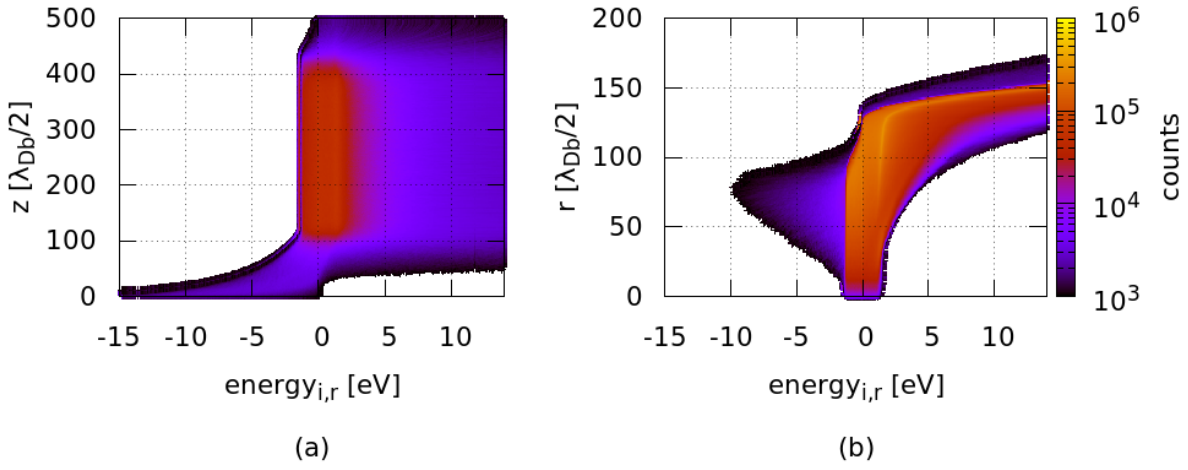

Figure 3.8: Ion energy distribution in r direction. (a) shows the averaged energy resolved for the vertical z axis and (b) for the radial r axis

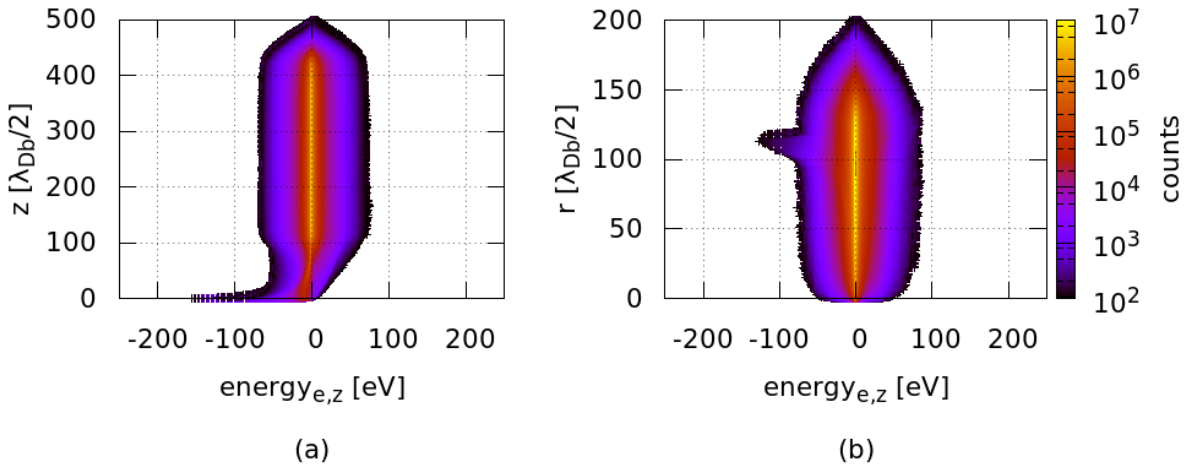

Figure 3.9: Electron energy distribution in z direction. (a) shows the averaged energy resolved for the vertical z axis and (b) for the radial r axis

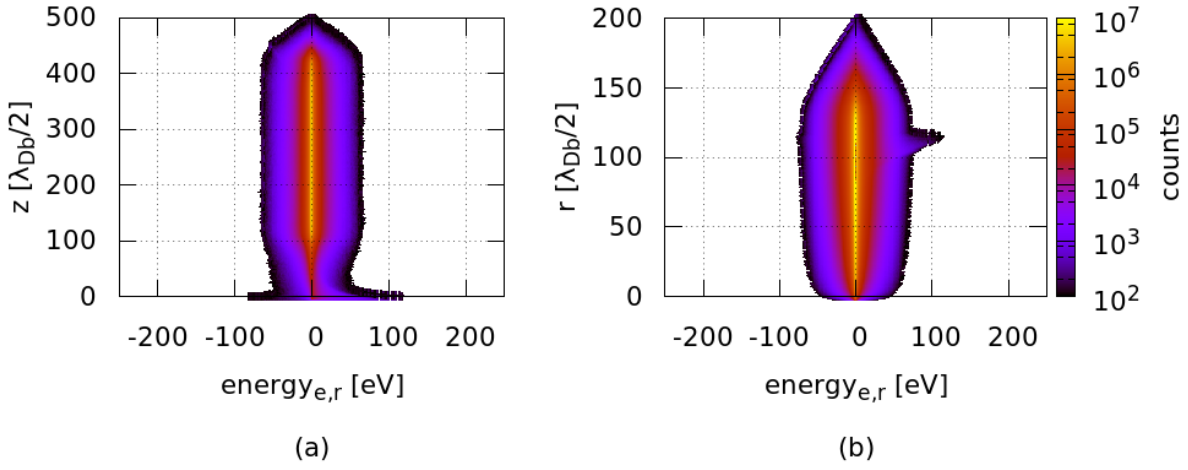

Figure 3.10: Electron energy distribution in r direction. (a) shows the averaged energy resolved for the vertical z axis and (b) for the radial r axis

4 Conclusion

In this thesis I successfully simulated electronegative capacitively coupled rf plasmas in one dimension under low pressure oxygen using the Particle-in-Cell method. Due to latest experimental results, showing a high-energy peak in the anion energy distribution depending on the used cathode material, secondary ion emission effects were additionally applied. Since the theoretical background of these surface effects is not given yet, an injection mechanism depending on impinging ions was implemented. With the model of SIE I was able to recreate and explain qualitatively the experimental measured high-energy peak of negative oxygen ions O^- at the anode. The simulation results yielded an additional low-energy peak in contradiction to the experiment. It could be shown that the peak forms due to the surface anions staying in the discharge and then colliding with neutrals in the sheaths. I then continued and varied the system parameters to get a quantitative understanding of the anion energy distribution function in respect to applied power, pressure and injection ratio η. The acquired results were very close to the experimental measurements except for the variation of the injection parameter η, which only slightly affected the resulting anion energy distributions. It was shown that due to the lack of asymmetry, which cannot be covered in an one-dimensional simulation, the injected anions stay in the discharge and then add up to a constant state, not influenced by the different chosen injection ratios η. The experiment otherwise states big differences for different cathode materials.
Therefore, a two-dimensional model was introduced, but the corresponding research is still at the beginning. With this two-dimensional model a micro discharge and an asymmetric ccrf discharge with argon as a working gas have been simulated. Especially, the influence of the asymmetry on the number density distribution and on the energy distribution could be observed. Through comparison it was shown that the one-dimensional model is a good approximation for the center of the discharge, except for the forming of a self-bias voltage. Due to runtime reasons an in depth study lays beyond the scope of this thesis.
The next step would be to implement oxygen as a working gas and apply physically motivated SIE in the two dimensional model. Then, one could apply different cathode materials to see the influence of different work functions on the anion O^- energy distribution function, which could not be obtained in one dimension.
To the best of my knowledge until now there do not exist any publications of two dimensional PIC simulations of low temperature laboratory plasmas yet. So the developed tool has still a lot of potential.

List of Figures

Bibliography

[1] U. Cvelbar, M. Mozetic, and M. Klansjek-Gunde. "Selective oxygen plasma etchin of coatings". In: *Plasma Science, IEEE* 3.2 (2005), pp. 236–237.

[2] M. Zeuner et al. "Sputter process diagnostics by negative ions". In: *Journal of Applied Physics* 83.10 (1998), pp. 5083–5086.

[3] S. Scheuer. "Plasmadiagnostische Untersuchungen zur Charakterisierung von Moden in elektronegativen RF-Plasmen". In: *Master thesis* (2015).

[4] H. Kawano and F. M. Page. "Experimental methods and techniques for negative-ion production ionization". In: *International Journal of Mass Spectrometry and Ion Physics* 50 (1983), pp. 1–33.

[5] J. Meichnser et al. "Nonthermal Plasma Chemistry and Physics". In: (2013).

Acknowledgments

I wish to thank the whole work group of Prof. Ralf Schneider, who put me in touch with this Master Thesis and helped me with good advice and support during this thesis.
They always had time to discuss current topics and to help me, no matter if it was about my thesis work or just for fun. A special thanks goes to Tabea Stegmaier which supported me morally and culinary especially during the last part of this thesis. Last but not least, thanks to my family who always backed me up no matter what and everyone else who supported me during this thesis.